

Chapter 2

Precoded Spatial Modulation-Aided Cooperative NOMA*

*Part of this work has been published as:

M. Hemanta Kumar, Sanjeev Sharma, M. Thottappan, and Kuntal Deka. “Precoded spatial modulation-aided cooperative NOMA”, *IEEE Communications Letters* 25, no. 6 (2021): 2053-2057.

2.1 Introduction

In this chapter, the focus is on how massive connectivity can be used to improve the performance of cell-edge users. To achieve this, a precoded spatial modulation aided cooperative NOMA, referred to as PC-NOMA, for MIMO downlink scenarios is proposed. The proposed model, the BS broadcasts three users' information over two-time slots: in the first slot, the two near users (NUs) receive the data through direct links, and in the second slot, the third user (far) receives the data indirectly from the near users. The precoded direct links' signal is superposed with the indirect link's signal in the broadcast phase at the BS. The indirect link's signal is decoded and forwarded to the direct link's user by using the SIC method in the cooperative phase.

The main contributions of the chapter is summarized as follows:

- The theoretical expressions of symbol error rate (SER) and mutual information (MI) under inter-user interference (IUI) are derived for the proposed PC-NOMA scheme, and also the impact of multiple transmitting and receiving antennas for precoded NUs is analyzed.
- The effect of transmitting and receiving antennas on the diversity order of users.
- Simulation results of PC-NOMA with better SER, diversity and sum-rate performances over conventional cooperative NOMA (CC-NOMA) for three users scenario are presented.
- Impact of multiple transmitting and receiving antennas with different precoding schemes are studied.

- Lastly, performances of PC-NOMA is compared with existing methods.

This chapter is organized as follows. Section 2.2 presents the proposed model of precoded SM-aided cooperative NOMA. Multiuser detection using SIC is addressed in Section 2.3. In Section 2.4, derived analytical expressions of the mutual information and symbol error rate. Analytical and simulation results are presented in Section 2.5 and the summary of the proposed work is discussed in Sections 2.6.

2.2 Proposed PC-NOMA System Model

In the proposed model, the users are divided into multiple clusters with three users in each cluster. The three users \mathcal{U}_1 , \mathcal{U}_2 and \mathcal{U}_3 of each cluster in C-NOMA system for downlink MIMO transmissions is shown in Figure 2.1. It is assumed that \mathcal{U}_1 and \mathcal{U}_2 are NUs, and user \mathcal{U}_3 is the far user (FU) to the BS in the proposed PC-NOMA model. The FU \mathcal{U}_3 has no direct link from the BS, as shown in Figure 2.1. BS and users have N_t and N_r antennas, respectively, and $N_t \geq N_r$ to reduce the IUI level and all the NUs work in half-duplex mode. The channels between the BS to direct link users \mathcal{U}_1 and \mathcal{U}_2 are denoted as \mathbf{H}_{B1} and $\mathbf{H}_{B2} \in \mathbb{C}^{N_r \times N_t}$, respectively. The cooperative phase channels among the three users \mathcal{U}_1 to \mathcal{U}_2 , \mathcal{U}_2 to \mathcal{U}_1 and \mathcal{U}_1 to \mathcal{U}_3 , \mathcal{U}_2 to \mathcal{U}_3 are denoted by \mathbf{h}_{21} , $\mathbf{h}_{12} \in \mathbb{C}^{N_r \times 1}$, and \mathbf{h}_{31} $\mathbf{h}_{32} \in \mathbb{C}^{N_r \times 1}$, respectively. All the channels considered are Rayleigh-flat fading channel which are independent and identically distributed (i.i.d) [65, 67, 70–74] with $\mathbf{H}_{Bt} \sim \mathcal{CN}(0, \sigma_t^2)$, $t = 1, 2$ and $\mathbf{h}_{lm} \sim \mathcal{CN}(0, \sigma_{lm}^2)$, $l = 1, 2, 3$, $m = 1, 2$, and $l \neq m$. The channel gain of NU is higher than the FU, i.e., $\sigma_t^2 \gg \sigma_{lm}^2$ [70]. The BS transmits the information of user \mathcal{U}_1 and \mathcal{U}_2 in *odd* ($2k+1$) and *even* ($2k$) time slot for $k = 0, 1, \dots$, respectively, while the information of \mathcal{U}_3 is transmitted in both *odd* ($2k+1$) and *even* ($2k$) time slots, as shown in Figure 2.1. The user \mathcal{U}_1 transmits information by modulating the receive

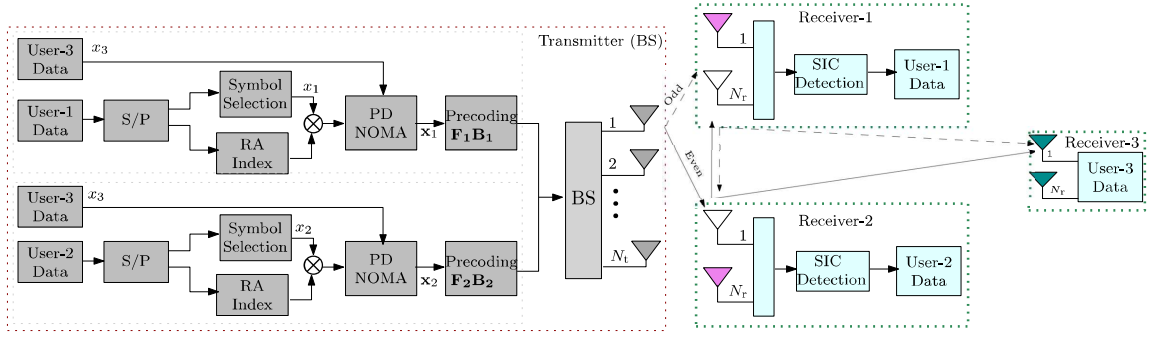


FIGURE 2.1: Proposed downlink PC-NOMA.

antennas (RA) index and constellation points jointly. Therefore, the first part of information bits is used to select the active index of RA and the remaining bits are mapped to modulate symbols. Hence, transmit vector, \mathbf{x}_1 is denoted as,

$$\mathbf{x}_1 = \left[\underbrace{0, \dots, 0}_{(j-1)\text{zeros}}, \mathcal{S}_1, \underbrace{0, \dots, 0}_{(N_r-j)\text{zeros}} \right]^T \in \mathbb{C}^{N_r \times 1}, \quad (2.1)$$

where, $\mathcal{S}_1 = \sqrt{\alpha_1 P_B} x_1(2k+1) + \sqrt{\alpha_3 P_B} x_3(2k+1)$ with $x_1(2k+1) \in \mathcal{X}_1$ and $x_3(2k+1) \in \mathcal{X}_3$ denotes the superimposed signal of \mathcal{U}_1 and \mathcal{U}_3 . \mathcal{X}_1 and \mathcal{X}_3 are constellations of user \mathcal{U}_1 and \mathcal{U}_3 , respectively. P_B is the total power available at the BS for signal transmission, and $\alpha_1 + \alpha_3 = 1$. The coefficients α_1 and α_3 are assigned according to channel gain condition of NUs and FU. The NUs channel gain is higher than the FU, therefore $\alpha_3 > \alpha_1$ [70].

In the PC-NOMA, \mathbf{x}_1 is precoded by a precoder matrix and is given as

$$\mathbf{x}_{\text{odd}} = \mathbf{F}_1 \mathbf{B}_1 \mathbf{x}_1 \quad (2.2)$$

where \mathbf{F}_1 is precoder for user \mathcal{U}_1 as

$$\mathbf{F}_1 = \begin{cases} \mathbf{H}_{B1}^H (\mathbf{H}_{B1} \mathbf{H}_{B1}^H)^{-1} \in \mathbb{C}^{N_t \times N_r} & \text{for ZF} \\ \mathbf{H}_{B1}^H (\mathbf{H}_{B1} \mathbf{H}_{B1}^H + N_r \sigma^2 \mathbf{I}_{N_r})^{-1} \in \mathbb{C}^{N_t \times N_r} & \text{for MMSE} \end{cases} \quad (2.3)$$

and \mathbf{B}_1 is normalized matrix for \mathcal{U}_1 as

$$\mathbf{B}_1 = \sqrt{\frac{1}{[(\mathbf{H}_{B1}\mathbf{H}_{B1}^H)^{-1}]}} \in \mathbb{C}^{N_r \times N_r}. \quad (2.4)$$

Similarly, users \mathcal{U}_2 and \mathcal{U}_3 information is transmitted in *even* ($2k$) time slot and transmit vector \mathbf{x}_2 is given as

$$\mathbf{x}_2 = [\underbrace{0, \dots, 0}_{(j-1)\text{zeros}}, \mathcal{S}_2, \underbrace{0, \dots, 0}_{(N_r-j)\text{zeros}}]^T \in \mathbb{C}^{N_r \times 1}, \quad (2.5)$$

where, $\mathcal{S}_2 = \sqrt{\alpha_2 P_B} x_2(2k) + \sqrt{\alpha_3 P_B} x_3(2k)$ with $x_2(2k) \in \mathcal{X}_2$ and $x_3(2k) \in \mathcal{X}_3$. The coefficients α_2 and α_3 are assigned according to the channel gain condition of NU \mathcal{U}_2 and FU \mathcal{U}_3 , and $\alpha_3 > \alpha_2$. The precoded vector \mathbf{x}_{even} for the *even* time-slot is given as,

$$\mathbf{x}_{\text{even}} = \mathbf{F}_2 \mathbf{B}_2 \mathbf{x}_2 \quad (2.6)$$

where, precoding matrix \mathbf{F}_2 for the user \mathcal{U}_2 is given as,

$$\mathbf{F}_2 = \begin{cases} \mathbf{H}_{B2}^H (\mathbf{H}_{B2} \mathbf{H}_{B2}^H)^{-1} \in \mathbb{C}^{N_t \times N_r} & \text{for ZF} \\ \mathbf{H}_{B2}^H (\mathbf{H}_{B2} \mathbf{H}_{B2}^H + N_r \sigma^2 \mathbf{I}_{N_r})^{-1} \in \mathbb{C}^{N_t \times N_r} & \text{for MMSE} \end{cases} \quad (2.7)$$

and \mathbf{B}_2 is the normalized matrix for \mathcal{U}_2 which is written as,

$$\mathbf{B}_2 = \sqrt{\frac{1}{[(\mathbf{H}_{B2}\mathbf{H}_{B2}^H)^{-1}]}} \in \mathbb{C}^{N_r \times N_r}. \quad (2.8)$$

Therefore, the BS transmits \mathbf{x}_{odd} and \mathbf{x}_{even} signals during both *odd* ($2k+1$) and *even* ($2k$) time-slots, respectively.

2.3 Multiuser Detection

In this section, signal detection for NUs and FU in the PC-NOMA is considered. At the *odd*-time slot, the received signal by the user \mathcal{U}_1 is expressed as,

$$\mathbf{y}_1 = \mathbf{H}_{B1}\mathbf{x}_{odd} + \mathbf{h}_{12} \odot \hat{x}_3^2(2k) + \mathbf{n}_1 \in \mathbb{C}^{N_r \times 1}, \quad (2.9)$$

where, \odot denotes the multiplication. $\hat{x}_3^2(2k)$ denotes the symbol of user \mathcal{U}_3 which is decoded in the *even*-time slot at the user \mathcal{U}_2 in cooperative mode. \mathbf{n}_1 denotes the additive white Gaussian noise (AWGN) vector of zero mean with covariance matrix of $N_0\mathbf{I}_{N_r}$, i.e., $\mathbf{n}_1 \sim \mathcal{CN}(0, N_0\mathbf{I}_{N_r})$. The user \mathcal{U}_1 receives desired signals from the BS along with IUI from the cooperative user \mathcal{U}_2 as given in (2.9). The SIC-based signal detection is used at \mathcal{U}_1 to decode $x_1(2k+1)$.

The maximum-likelihood (ML) detection of user \mathcal{U}_3 at \mathcal{U}_1 is expressed as,

$$\hat{x}_3^1(2k+1) = \arg \min_{x_3(2k+1) \in \mathcal{X}_3, j \in \{1, \dots, N_r\}} \|\mathbf{y}_1 - \mathbf{H}_{B1}\mathbf{x}_{odd}^3\|_2^2, \quad (2.10)$$

where, $\hat{x}_3^1(2k+1)$ denotes the decoded symbol of user \mathcal{U}_3 at user \mathcal{U}_1 in the *odd*-time slot and $\mathbf{x}_{odd}^3 = \mathbf{F}_1\mathbf{B}_1\mathbf{x}_3^1$ with $\mathbf{x}_3^1 = \underbrace{[0, \dots, 0]_{(j-1)}}_{(j-1)}, (\sqrt{\alpha_3 P_B}x_3), \underbrace{[0, \dots, 0]_{(N_r-j)}}_{(N_r-j)}$. In SIC-based detection, \mathcal{U}_3 signal is subtracted from the received signal \mathbf{y}_1 which is written as,

$$\mathbf{y}_{1,\text{SIC}} = \mathbf{y}_1 - \mathbf{H}_{B1}\hat{\mathbf{x}}_{odd}, \quad (2.11)$$

where, $\hat{\mathbf{x}}_{odd} = \mathbf{x}_{odd}^3$ with $x_3 = \hat{x}_3^1(2k+1)$. After the SIC, the ML detection of user \mathcal{U}_1 is given as,

$$\hat{x}_1(2k+1) = \arg \min_{x_1(2k+1) \in \mathcal{X}_1, j \in \{1, \dots, N_r\}} \|\mathbf{y}_{1,\text{SIC}} - \mathbf{H}_{B1}\mathbf{x}_{odd}^1\|_2^2, \quad (2.12)$$

where, $\mathbf{x}_{odd}^1 = \mathbf{F}_1 \mathbf{B}_1 \mathbf{x}_1^1$ with $\mathbf{x}_1^1 = [0, \dots, 0, \underbrace{(\sqrt{\alpha_1 P_B} x_1)}_{(j-1)}, \underbrace{0, \dots, 0}_{(N_r-j)}]$. Therefore, both \mathcal{U}_1 and \mathcal{U}_3 users' symbols are decoded as $\hat{x}_1(2k+1)$ and $\hat{x}_3^1(2k+1)$, respectively at user-1 in the *odd*-time slot.

Similarly, detection for user \mathcal{U}_2 and \mathcal{U}_3 is carried out at user-2 in the *even*-time slot and the received signal at \mathcal{U}_2 is given as,

$$\mathbf{y}_2 = \mathbf{H}_{B2} \mathbf{x}_{even} + \mathbf{h}_{21} \odot \hat{x}_3(2k-1) + \mathbf{n}_2 \in \mathbb{C}^{N_r \times 1}, \quad (2.13)$$

where, $\mathbf{n}_2 \sim \mathcal{CN}(0, N_0 \mathbf{I}_{N_r})$ is AWGN and $\hat{x}_3^1(2k-1)$ is \mathcal{U}_3 's symbol which is decoded at user-1 in the *odd*-time slot. Similarly, the ML detection of user \mathcal{U}_3 at user-2 is expressed as,

$$\hat{x}_3^2(2k) = \arg \min_{x_3(2k) \in \mathcal{X}_3, j \in \{1, \dots, N_r\}} \|\mathbf{y}_2 - \mathbf{H}_{B2} \mathbf{x}_{even}^3\|_2^2, \quad (2.14)$$

where, $\hat{x}_3^2(2k)$ denotes the decoded symbol of user \mathcal{U}_3 at user \mathcal{U}_2 in the *even*-time slot and $\mathbf{x}_{even}^3 = \mathbf{F}_2 \mathbf{B}_2 \mathbf{x}_3^2$ with $\mathbf{x}_3^2 = [0, \dots, 0, \underbrace{(\sqrt{\alpha_3 P_B} x_3)}_{(j-1)}, \underbrace{0, \dots, 0}_{(N_r-j)}]$. In SIC based detection, \mathcal{U}_3 signal is subtracted from the received signal \mathbf{y}_2 which is given as

$$\mathbf{y}_{2,\text{SIC}} = \mathbf{y}_2 - \mathbf{H}_{B2} \hat{\mathbf{x}}_{even}, \quad (2.15)$$

where, $\hat{\mathbf{x}}_{even} = \mathbf{x}_{even}^3$ with $x_3^2 = \hat{x}_3^2(2k)$. After the SIC, the ML detection of user \mathcal{U}_2 is given as

$$\hat{x}_2(2k) = \arg \min_{x_2(2k) \in \mathcal{X}_2, j \in \{1, \dots, N_r\}} \|\mathbf{y}_{2,\text{SIC}} - \mathbf{H}_{B2} \mathbf{x}_{even}^2\|_2^2, \quad (2.16)$$

where, $\mathbf{x}_{even}^2 = \mathbf{F}_2 \mathbf{B}_2 \mathbf{x}_2^2$ with $\mathbf{x}_2^2 = [0, \dots, 0, \underbrace{(\sqrt{\alpha_2 P_B} x_2)}_{(j-1)}, \underbrace{0, \dots, 0}_{(N_r-j)}]$. Therefore, both users \mathcal{U}_2 and \mathcal{U}_3 symbols are decoded as $\hat{x}_2(2k)$ and $\hat{x}_3^2(2k)$, respectively at user-2 in the *even*-time ($2k$) slot.

The \mathcal{U}_1 and \mathcal{U}_2 transmit the FU's information in the *odd* and *even*-time slot, respectively. Therefore, the transmit signal of FU is given as

$$x_3(2k+1) = \sqrt{\mathcal{P}_0}\hat{x}_3(2k+1) \text{ and } x_3(2k) = \sqrt{\mathcal{P}_e}\hat{x}_3(2k) \quad (2.17)$$

at the \mathcal{U}_1 and \mathcal{U}_2 , respectively. \mathcal{P}_0 and \mathcal{P}_e denote the transmit power at \mathcal{U}_1 and \mathcal{U}_3 , respectively. The received signals at \mathcal{U}_3 in *odd* and *even* time slots are described as,

$$\mathbf{y}_3(p) = \mathbf{h}_{3p} \odot x_3(p) + \mathbf{n}_3(p) \in \mathbb{C}^{N_r \times 1}, p = 2k, 2k+1, \quad (2.18)$$

where, $n_3(p)$ denotes the AWGN and the ML detection of \mathcal{U}_3 is considered in (2.18).

2.4 Sum Rate Performance Analysis

In this section, the MI and SER performance analysis of the proposed PC-NOMA are considered.

2.4.1 Mutual Information Analysis

In the PC-NOMA, the direct link user \mathcal{U}_1 experiences IUI. Therefore, after employing SIC the \mathcal{U}_1 s received signal is expressed as,

$$\mathbf{y}_1 = \mathbf{H}_{B1}\boldsymbol{\eta}_1 + \mathbf{h}_{12} \odot \hat{x}_3(2k) + \mathbf{n}_1, \quad (2.19)$$

where, $\boldsymbol{\eta}_1 = \mathbf{x}_{odd}^1$. which $\boldsymbol{\eta}_1$ consists of active RA's whose indices are $\mathbf{e}_j \in \mathbb{R}^{N_r \times 1}, j = 1, \dots, N_r$, which is j^{th} column of identity matrix, \mathbf{I}_{N_r} . Further, $x_1 \in \mathcal{X}_1$ is an M level

$$\begin{aligned}
p(\mathbf{y}_1|\mathbf{B}_j, x_1) &= \frac{1}{\sqrt{2\pi\sigma_{\mathbf{w}_a}^2}} \exp\{-\Psi\}, \\
p(\mathbf{y}_1|x_1) &= \sum_{j=1}^{N_r} \frac{1}{\sqrt{2\pi\sigma_{\mathbf{w}_a}^2}} \exp\{-\Psi\}, p(\mathbf{y}_1|\mathbf{B}_j) = \sum_{x_1 \in \mathcal{X}_1} \frac{1}{\sqrt{2\pi\sigma_{\mathbf{w}_a}^2}} \exp\{-\Psi\} \\
p(\mathbf{y}_1, \mathbf{B}_j|x_1) &= \frac{1}{N_r} \frac{1}{\sqrt{2\pi\sigma_{\mathbf{w}_a}^2}} \exp\{-\Psi\}, p(\mathbf{y}_1) = \frac{1}{MN_r} \sum_{x_1 \in \mathcal{X}_1} \sum_{j=1}^{N_r} \frac{1}{\sqrt{2\pi\sigma_{\mathbf{w}_a}^2}} \exp\{-\Psi\}, \\
\text{where } \Psi &= \frac{\|\mathbf{y}_1 - \mathbf{B}_j \sqrt{\alpha_1 P_B} x_1\|^2}{2\sigma_{\mathbf{w}_a}^2}
\end{aligned} \tag{2.22}$$

modulated symbols of \mathcal{U}_1 , therefore (2.19) can be rewritten as,

$$\mathbf{y}_1 = \mathbf{B}_1 \mathbf{e}_j \sqrt{\alpha_1 P_B} x_1 + \mathbf{w}_a = \mathbf{B}_j \sqrt{\alpha_1 P_B} x_1 + \mathbf{w}_a, \tag{2.20}$$

where, \mathbf{w}_a is an equivalent received IUI plus noise signal at \mathcal{U}_1 , which is represented as $\mathbf{w}_a = \mathbf{h}_{12} \odot \hat{x}_3(2k) + \mathbf{n}_1$ and \mathbf{B}_j is an activated diagonal matrix of RAs given for the x_1 . The MI between the discrete random input, x_1 and the channel output of \mathbf{y}_1 for \mathcal{U}_1 can be decomposed into MI for an active RA and modulated symbols which is given as [67] as,

$$I(x_1, \mathbf{B}_j; \mathbf{y}_1) = I(\mathbf{B}_j; \mathbf{y}_1|x_1) + I(x_1; \mathbf{y}_1), \tag{2.21}$$

where, $I(\mathbf{B}_j; \mathbf{y}_1|x_1)$ represents the average conditional MI between \mathbf{y}_1 and \mathbf{B}_j for the given x_1 and $I(x_1; \mathbf{y}_1)$ denotes the average MI between x_1 and \mathbf{y}_1 . The conditional probability density functions (PDFs) of signal \mathbf{y}_1 are given in (2.22), where $\sigma_{\mathbf{w}_a}^2$ denotes the variance of \mathbf{w}_a .

By using the conditional PDFs in (2.22), the average conditional MI, $I(\mathbf{B}_j; \mathbf{y}_1|x_1)$ and average MI $I(x_1; \mathbf{y}_1)$ evaluate as given in (2.23), where $\mathbf{d}_j^{j'} = (\mathbf{B}_j - \mathbf{B}_{j'})x_1$ and $\mathbf{d}_{x_1, j}^{x_{1'}, j'} = (\mathbf{B}_j x_1 - \mathbf{B}_{j'} x_{1'})$.

$$\begin{aligned}
I(\mathbf{B}_j; \mathbf{y}_1 | x_1) &= \log_2(N_r) - \frac{1}{MN_r} \sum_{x_1 \in \mathcal{X}_1} \sum_{j=1}^{N_r} \mathbb{E}[\mathbf{w}_a] \log_2 \left[\sum_{j'=1}^{N_r} \exp \left\{ \frac{\|\mathbf{w}_a\|^2 - \|\mathbf{w}_a + \mathbf{d}_j^{j'}\|^2}{2\sigma_{\mathbf{w}_a}^2} \right\} \right], \text{ and} \\
I(x_1; \mathbf{y}_1) &= \log_2(M) - \frac{1}{MN_r} \sum_{x_1 \in \mathcal{X}_1} \sum_{j=1}^{N_r} \mathbb{E}[\mathbf{w}_a] \log_2 \left[\frac{\sum_{x_{1'} \in \mathcal{X}_1} \sum_{j'=1}^{N_r} \exp \left\{ -\frac{\|\mathbf{w}_a + \mathbf{d}_{x_{1'}, j'}^{x_{1'}, j'}\|^2}{\sigma_{\mathbf{w}_a}^2} \right\}}{\sum_{j=1}^{N_r} \exp \left\{ -\frac{\|\mathbf{w}_a + \mathbf{d}_{x_1, j}^{x_1, j}\|^2}{2\sigma_{\mathbf{w}_a}^2} \right\}} \right]
\end{aligned} \tag{2.23}$$

Plugging (2.23) into (2.21), the MI for \mathcal{U}_1 is obtained as,

$$\begin{aligned}
I(x_1, \mathbf{B}_j; \mathbf{y}_1) &= \log_2(MN_r) - \frac{1}{MN_r} \sum_{x_1 \in \mathcal{X}_1} \sum_{j=1}^{N_r} \mathbb{E}[\mathbf{w}_a] \\
&\left(\log_2 \sum_{x_{1'} \in \mathcal{X}_1} \sum_{j'=1}^{N_r} \exp \left(-\frac{\|\mathbf{w}_a + \mathbf{d}_{x_{1'}, j'}^{x_{1'}, j'}\|^2 - \|\mathbf{w}_a\|^2}{2\sigma_{\mathbf{w}_a}^2} \right) \right),
\end{aligned} \tag{2.24}$$

A similar procedure can be used to derive the MI for \mathcal{U}_2 .

The FU \mathcal{U}_3 received information from user \mathcal{U}_2 and user \mathcal{U}_1 in *odd* and *even* time slots, respectively. Its channels are $\mathbf{h}_{32} = \mathbf{h}_{31} = \mathbf{h}_p$. Therefore, the MI can be represented as $I(x_3; y_3, h_p)$ [75],

$$I(x_3; \mathbf{y}_3, \mathbf{h}_p) = \frac{1}{2N_r} \sum_{p=1}^{N_r} [\log_2 (1 + \mathcal{P}_{\text{snr}} \|\mathbf{h}_p\|^2)], \tag{2.25}$$

where, \mathcal{P}_{snr} is average SNR, which is defined as the $\mathcal{P}_{\text{snr}} = \frac{\mathcal{P}}{\sigma_{n_3}^2}$, here $\mathcal{P} = \mathcal{P}_o = \mathcal{P}_e$ is the power transmits by relay nodes and $\sigma_{n_3}^2$ is the noise variance of \mathbf{n}_3 at *odd* and *even* time-slots. The sum-rate of the proposed PC-NOMA for the three user's model is given as,

$$R_{\text{sum}} = 2I_{\text{LB}}(x, \mathbf{B}; \mathbf{y}) + \frac{1}{2N_r} \sum_{p=1}^{N_r} (\log_2 (1 + \mathcal{P}_{\text{snr}} \|\mathbf{h}_p\|^2)) \tag{2.26}$$

$I_{\text{LB}}(x, \mathbf{B}; \mathbf{y})$ denotes the lower bound of MI of a NU which is given as,

$$\log_2 \left(\frac{MN_r}{e} \right) - \frac{1}{(MN_r)} \times \sum_{x_1 \in \mathcal{X}_1} \sum_{j=1}^{N_r} \log_2 \left(\sum_{x_{1'} \in \mathcal{X}_1} \sum_{j'=1}^{N_r} e^{-\frac{(\mathbf{d}_{x_{1'}, j'})^2}{4\sigma_{\mathbf{w}_a}^2}} \right).$$

2.4.2 SER Analysis

In the proposed PC-NOMA, NUs have strong IUI in broadcasting phase and the IUI at \mathcal{U}_1 and \mathcal{U}_2 is represented as,

$$\mathcal{I}_1 = \mathbf{h}_{12} \odot \sqrt{\mathcal{P}_e} \hat{x}_3(2k) + \mathbf{n}_1 \text{ and } \mathcal{I}_2 = \mathbf{h}_{21} \odot \sqrt{\mathcal{P}_o} \hat{x}_3(2k-1) + \mathbf{n}_2. \quad (2.27)$$

The equivalent distribution of IUI for the direct-link NUs is given by

$$\mathcal{I}_m \sim \mathcal{CN}(0, \zeta_m^2 + \sigma_{n_m}^2), m = 1 \text{ and } 2, \quad (2.28)$$

where, ζ_1^2 and ζ_2^2 represent variance of terms $(\mathbf{h}_{12} \odot \sqrt{\mathcal{P}_e} \hat{x}_3(2k))$ and $(\mathbf{h}_{21} \odot \sqrt{\mathcal{P}_o} \hat{x}_3(2k-1))$, respectively. Further, SER in the PC-NOMA of \mathcal{U}_1 and \mathcal{U}_2 can be approximated as [67]

$$f_{\text{SER}}^{(1)} \approx \text{erfc} \left(\frac{\zeta_{\mathcal{U}_1}^2}{\zeta_1^2 + \sigma_{n_1}^2} \right), f_{\text{SER}}^{(2)} \approx \text{erfc} \left(\frac{\zeta_{\mathcal{U}_2}^2}{\zeta_2^2 + \sigma_{n_2}^2} \right), \quad (2.29)$$

where, $\text{erfc}(\cdot)$ is the complementary error function and $\zeta_{\mathcal{U}_1}^2$ and $\zeta_{\mathcal{U}_2}^2$ are variance of desired received signals from the BS. The \mathcal{U}_3 , is free from IUI, therefore its SER can be expressed as

$$f_{\text{SER}}^{(3)} \approx \text{erfc} \left(\frac{\zeta_{\mathcal{U}_3}^2}{\sigma_{n_3}^2} \right) \quad (2.30)$$

where $\zeta_{\mathcal{U}_3}^2$ is variance of the desired signals of \mathcal{U}_3 , which is received from \mathcal{U}_2 and \mathcal{U}_1 in the *odd* and *even* time slots, respectively.

2.5 Simulation Results and Discussion

In this section, the simulation results are shown to demonstrate the effectiveness of the proposed PC-NOMA for three users. The SER and sum-rate performance metrics are evaluated for the PC-NOMA system. In simulations, the power coefficients $\alpha_1 = 0.2$, $\alpha_2=0.2$ and $\alpha_3 = 0.8$ and the total power $P_B = 1$ unit are considered. Further, $\mathcal{P}_o = \mathcal{P}_e = 0.2$ unit is assumed, and all users and BS are frame synchronized.

The average SER performance of NU \mathcal{U}_1 ¹ and FU \mathcal{U}_3 are analyzed as shown in Figure 2.2. The BS, and \mathcal{U}_1 and \mathcal{U}_3 are equipped with $N_t = 8, 4$ and $N_r = 2$ antennas, respectively with quadrature phase-shift keying (QPSK) modulation. It is observed from (Figure 2.2) that as N_t increases, \mathcal{U}_1 's SER performance is improved due to effective IUI mitigation. Further, theoretical (“Theo”) results are compared with the simulated results closely match, as shown in Figure 2.2, which validates the derived results. At high SNR, the SER performance of \mathcal{U}_1 (4×2) is limited by IUI, therefore, an error floor is observed in SER.

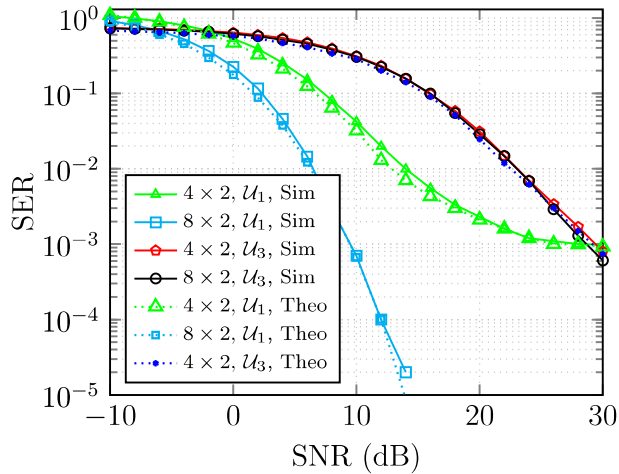


FIGURE 2.2: Theoretical and numerical results of average SER of the PC-NOMA with QPSK transmission for NU \mathcal{U}_1 and FU \mathcal{U}_3 .

¹User-2 has the same performance as \mathcal{U}_1 due to symmetry.

In Figure 2.3, the average SER performance of the proposed PC-NOMA and CC-NOMA [70] with binary phase-shift keying (BPSK) are shown. The PC-NOMA (“PC”) has better performance than the CC-NOMA (“CC”), as observed in Figure 2.3 due to IUI mitigation. The signal detection at \mathcal{U}_1 is done in the presence of IUI (2.9), therefore, at high SNR, the SER mainly depends on the IUI level. Hence, presence of IUI saturates SER at high SNR, which results in error floor for \mathcal{U}_1 . Further, FU \mathcal{U}_3 ’s detection is free from any IUI (2.18). Therefore, SER does not saturate at high SNR in the PC-NOMA, unlike in the CC-NOMA, as shown in Figure 2.3. Furthermore, QPSK performance is degraded as compared to the BPSK due to interference, as observed in Figure 2.3.

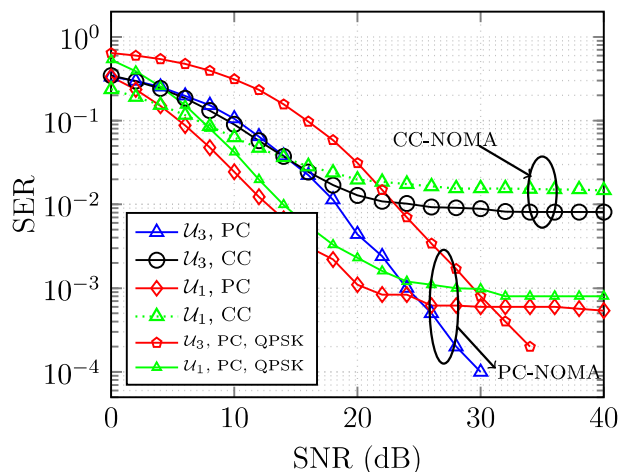


FIGURE 2.3: Average SER performance of NU \mathcal{U}_1 and FU \mathcal{U}_3 with $N_t = 4$ and $N_r = 2$.

Next, the impact of transmit and receive antennas are analyzed for the PC-NOMA as shown in Figure 2.4. The SER performance is improved as the number of transmitter antennas is increased for the fixed N_r due to reduced IUI level, as observed in Figure 2.4. Further, a higher value of N_r degrades the SER performance at fixed N_t due to higher IUI level, as shown in Figure 2.4. Therefore, higher diversity order in the PC-NOMA is achieved while considering higher N_t value. Further, MMSE precoding has better performance than ZF in PC-NOMA (Figure 2.4) due to noise regularization in

precoding. ZF is lower computational complexity compared to MMSE. An antenna grouping (AG)-PSM [67] has very less diversity as compared to PC-NOMA, as shown in Figure 2.4.

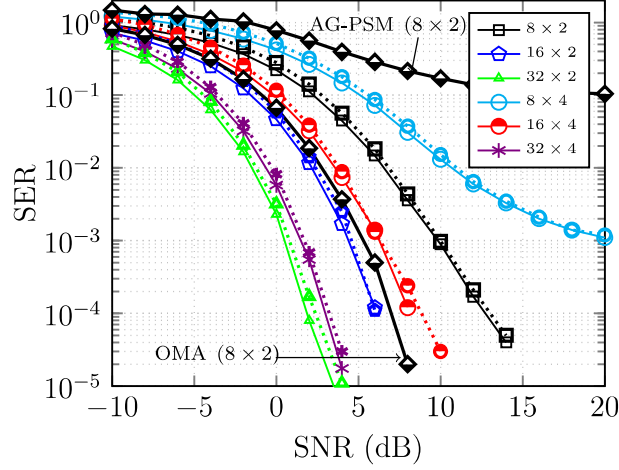


FIGURE 2.4: Average SER performance of NU \mathcal{U}_1 for different transmit $N_t = 8, 16, 32$ and receive $N_r = 2, 4$ antennas for QPSK modulation. Solid and dotted lines denote the performance of MMSE and ZF precoding, respectively.

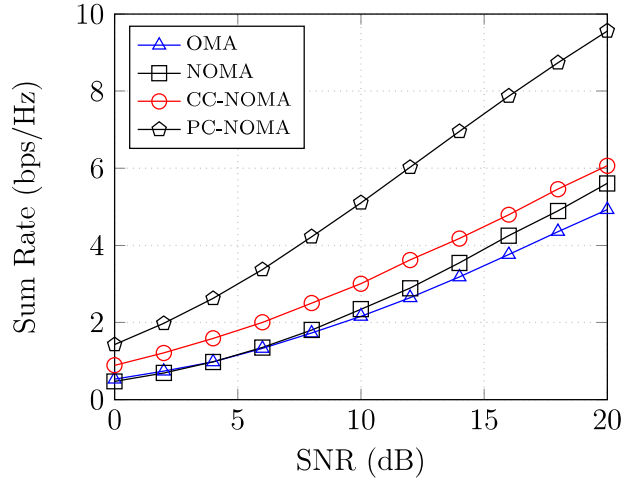


FIGURE 2.5: The sum rate vs SNR performance for $N_t = 4$ and $N_r = 2$.

The sum-rate performance of the PC-NOMA, CC-NOMA, OMA, and NOMA is shown in Figure 2.5. The PC-NOMA has a better sum rate performance than the CC-NOMA due to the interference mitigation. The power splitting of 0.2 and 0.8 is

considered between NU and FU in the sum rate calculation. CC-NOMA has better a sum-rate than the NOMA system, as observed in Figure 2.5.

The summary of the results proposes that the performance of the proposed PC-NOMA system is better than that of CC-NOMA, NOMA, and OMA. Furthermore, it supports more users in each cluster.

2.6 Summary

In this chapter, a PC-NOMA system of three users for the downlink MIMO transmission has been proposed and in which NUs information is transmitted using the index of receiving antenna and constellation points. Moreover, MI and SER expressions are derived for users in the PC-NOMA over Rayleigh flat fading channels. The proposed PC-NOMA achieved better SER, diversity order, and higher the sum-rate as compared to CC-NOMA. The impact of the number of transmitting and receiving antennas and modulation order are also studied in the PC-NOMA. Further, the simulation results established that a higher number of antennas at BS reduces IUI in PC-NOMA. Furthermore, it was observed that the latency is more in the relay model which should be addressed to make it suitable for next-generation wireless communication with low latency and high spectral efficiency. one of the solutions to address the aforementioned problem is to use a reconfigurable channel environment with a reconfigurable intelligent surface as follows in Chapter 3.